Spin-glass behavior in mechanically milled crystalline GdN

D. X. Li,* K. Sumiyama, and K. Suzuki
Institute for Materials Research, Tohoku University, Sendai, 980-77 Japan

T. Suzuki
Department of Physics, Tohoku University, Sendai, 980-77 Japan

(Received 24 September 1996)

Concentrated spin-glass behavior is discovered in a mechanically milled crystalline compound GdN. We report on measurements of magnetic relaxation and both ac and dc magnetic susceptibility at temperatures between 2 and 300 K in a magnetic field up to 5 T. Both ac and dc magnetic susceptibility measurements show a peak at freezing temperatures T_f that strongly depends on the frequency and amplitude of the applied magnetic field. The magnetic relaxation measurement shows a slow decay of the remanent magnetization with time below T_f, which is well described by an exponential function in a long time scale and a reciprocal proportion function in a short time scale. The results strongly suggest that spin-glass behaviors exist in mechanically milled crystalline compound GdN with the magnetic element as high as 50 at. %. [S0163-1829(97)01310-6]

I. INTRODUCTION

A spin glass is a particular type of magnetic system in which no conventional long-range order (of ferromagnetic or antiferromagnetic type) can be established. Nevertheless this system exhibits a ''freezing transition'' to a new kind of ''ordered'' state in which the magnetic moments are frozen in random directions. Since the experimental evidence of the spin-glass behavior found by Cannella and Mydosh,[1] numerous examples of spin glass have been discovered,[2–6] and there has been a continuous interest in trying to understand their physical properties. A necessary prerequisite for a spin glass is structural disorder of atoms (or clusters). Structural disorder achieved by either decrystallizing the materials or random occupation of crystal sites is common in spin-glass systems. By rapid quenching or sputtering techniques, spin-glass states are realized in amorphous alloys whose magnetic element content is up to about 70 at. %, such as $Gd_{0.37}Al_{0.63}$,[7] $(Fe_xNi_{1-x})_{75}P_{16}B_6Al_3$,[8] and $(Fe_xMn_{1-x})_{75}P_{16}B_6Al_3$.[9] Using the diluting method, spin-glass states are also obtained with a rather low content of magnetic elements (in the range 10^{-3}–10^{-1}). $Au_{1-x}Fe_x$ and $Cu_{1-x}Mn_x$ are the typical examples. In recent years, the mechanical milling technique has been used as a method to realize spin glasses. The first spin glass discovered by Zhou and Bakker in ball-milled materials is amorphous CoGe,[10,11] and recently, they succeeded in realizing a crystalline spin-glass $GdAl_2$ (Ref. 5) with the magnetic element content of 33 at. %.

In this paper, we describe the spin-glass behaviors in a single-phase crystalline compound GdN produced by high-energy ball milling (hereafter noted as bm-GdN). Since the magnetic element content in this system is as high as 50 at.%, we call this bm-GdN a concentrated spin-glass system.

GdN with the NaCl-type crystal structure is a typical low carrier, strongly correlated electron system, revealing mysterious magnetic properties. The band-structure calculation[12] suggests a semiconducting character for GdN. However, experimental results[13] indicate GdN to be semimetallic. The magnetic structure of GdN has also given rise to much controversy. Many authors[14–16] have reported a ferromagnetic transition at 65–75 K and a paramagnetic Curie temperature of 70–90 K for GdN. Based on magnetization and initial susceptibility measurements, Wachter and Kaldis[13] claimed GdN at low fields to be antiferromagnetic with a Néel temperature $T_N = 40$ K. They stated that GdN would be an antiferromagnet in zero field, if the carrier concentration in GdN is less than 10^{-3} per Gd atom. With increasing the carrier concentration, an oscillatory Ruderman-Kittel-Kasuya-Yosida interaction is superimposed on an antiferromagnetic superexchange interaction and GdN changes from the above-mentioned antiferromagnetic state to another antiferromagnetic one via a ferromagnetic state. Previously, we reported that GdN with a $^8S_{7/2}$ ground state is an exchange-dominating magnetic system.[17] Intense competition between ferromagnetic and antiferromagnetic interactions exist in GdN, and thus the magnetic structure of GdN is very sensitive to its carrier concentration, $4f$ energy level, lattice constant, and lattice defects. Different preparation methods lead to GdN samples with different degrees of stoichiometry, and therefore with different carrier concentrations. This may be why GdN can exist as a ferromagnet as well as an antiferromagnet at low fields, as shown by many authors. In this context, if we can make the Gd ions randomly occupying the crystal sites in GdN by mechanical milling, the ferromagnetic and antiferromagnetic interactions between nearest-neighbor Gd ions would coexist, and thus the concentrated spin-glass behavior would be observed in bm-GdN.

II. EXPERIMENTAL METHODS

It is difficult to obtain a stoichiometric GdN sample due to the high melting point and high vapor pressure. We applied a high-pressure method to prepare the starting compound GdN by using a hot isostatic pressure furnace. Flakes of Gd metal

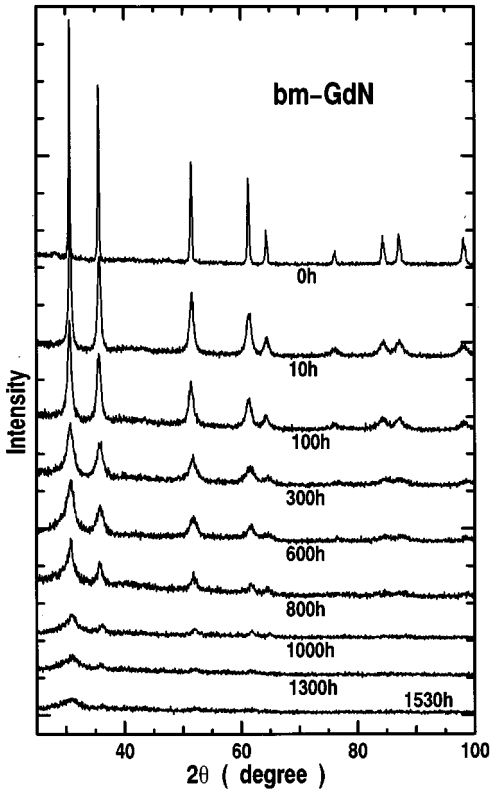

FIG. 1. X-ray diffraction patterns of bm-GdN samples after milling for typical periods.

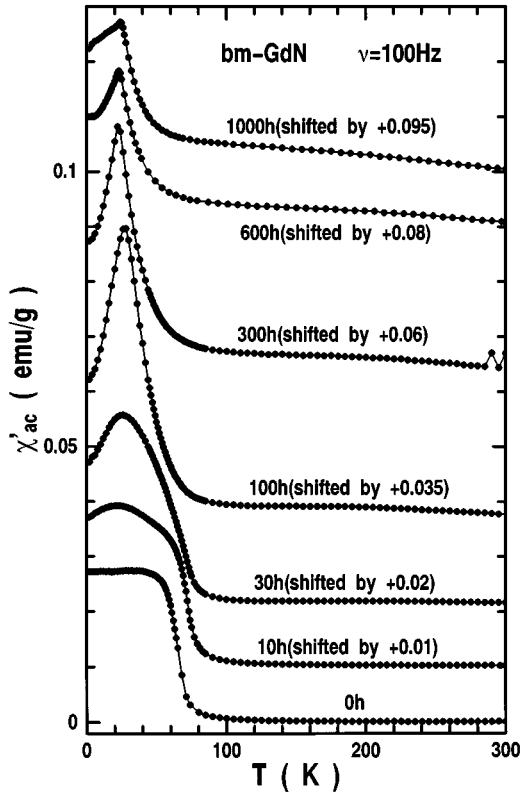

FIG. 2. Temperature dependence of the real part of the ac susceptibility of bm-GdN after milling for typical periods. A frequency of 100 Hz was used.

of 99.9% purity in an open tungsten crucible were directly reacted with nitrogen at 1600 °C and a N_2 pressure of 1300 atm for 3 h. X-ray diffraction patterns showed a single phase with the NaCl structure for the crude compound GdN prepared in this way. Ball milling was carried out in a hardened steel vial, in which the powder sample and stainless ball with the weight ratio of 1:7 were sealed in argon atmosphere. Chemical analysis indicated that the increase of impurity (mainly being Fe atoms) in the bm-GdN sample with milling time was about 0.8 wt. % per 100 h. The ac and dc susceptibilities (magnetization) were measured using a superconducting quantum interference device operating in the temperature range $2 \leqslant T \leqslant 300$ K, magnetic field range $0 \leqslant H \leqslant 5$ T, and frequency range $0.01 \leqslant \nu \leqslant 1000$ Hz.

III. EXPERIMENTAL RESULTS

Figure 1 illustrates the x-ray diffraction patterns of the crude GdN and bm-GdN samples milled for different times. High-energy ball milling results in broadening of all Bragg peaks and disappearance of a few diffraction lines with increasing the milling time. These features are ascribed to effects of chemical disorder, internal stresses, and the refinement of crystalline size as observed in mechanically milled compounds.[5] Several Bragg peaks can still be observed after milling for 1000 h. After 1530 h of milling, however, only a broad peak with a very small intensity appears, and the material seems to reach an amorphous state. Figure 2 shows the temperature dependence of the real part $\chi'(\nu,T)$ of ac susceptibility, $\chi_{\rm ac}$, measured in a frequency of $\nu = 100$ Hz for bm-GdN after typical periods of milling. Before milling, compound GdN shows the ferromagnetic behavior with a Curie temperature $T_C = 58$ K and the paramagnetic Curie temperature $\theta_P = 81$ K. These agree with our specific heat measurements.[17] As the milling time increases, this ferromagnetic character decreases and disappears after 100 h of milling. On the other hand, starting from 10 h of milling, another anomalous peak appears at about 22 K, much lower than $T_C = 58$ K, indicating the formation of a new magnetic phase. The peak intensity increases with milling time up to 100 h of milling, indicating the homogenization and the increase of the amount of this new magnetic phase. After 100 h of milling, the peak intensity decreases with milling time up to 1000 h. In contrast to the change of the peak intensity, the change of peak temperature with milling time is not so evident up to 1000 h of milling. The highest peak temperature is observed at 27 K after 100 h of milling with the highest peak intensity. As discussed later, this anomalous peak in bm-GdN is attributed to a spin-glass transition. After 1530 h of milling, however, the material seems to reach an amorphous state (see Fig. 1), and two peaks, a small peak at about 10 K and a large and broad peak at around 80 K, were observed in the $\chi' - T$ curves. These phenomena will be discussed in a separate paper. In this paper, we focus our attention on the spin-glass behavior of the bm-GdN sample. Because all the samples milled from 100 to 1000 h exhibit similar behavior, we will present the characteristic results obtained for a typical sample milled for 600 h (hereafter noted as bm-600h-GdN).

Spin glass is characterized by a cusp in ac susceptibility at freezing temperature T_f. T_f depends on the frequency of the

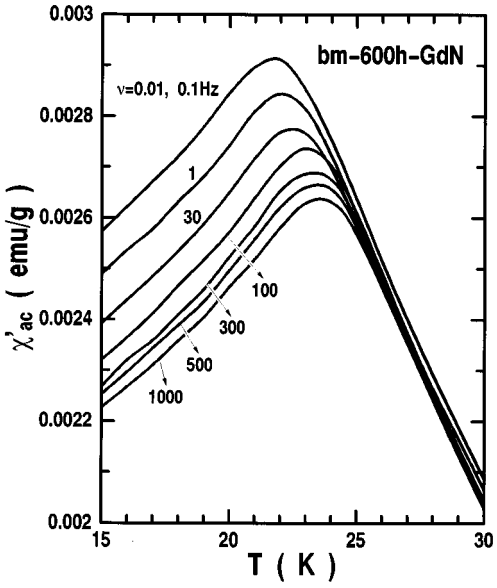

FIG. 3. Temperature dependence of the real part of the ac susceptibility of the bm-600h-GdN sample measured at a different frequency ν of the applied ac field.

applied magnetic field. The ''true'' T_f should therefore be estimated by extrapolation to the dc limit. Figure 3 shows the temperature dependence of $\chi'(\nu,T)$ of bm-600h-GdN measured under different frequencies. It is clear that a sharp cusp at $T_f=21.7$ K appears under a frequency of 0.1 Hz, and below this frequency χ' is almost frequency independent, indicating that a true equilibrium limit $\chi(0)$ has been reached. With increasing the frequency, the peak intensity decreases, while the peak temperature increases. The frequency dependence of the peak temperature is depicted in Fig. 4, the $T_f(\nu)$ data can be fitted fairly well by the following expression:

$$T_f(\nu)=T_0e^{-a/(\nu+b)}, \tag{1}$$

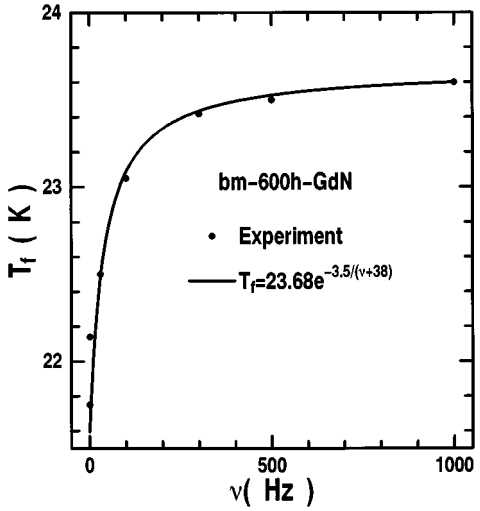

FIG. 4. Freezing temperature $T_f(\nu)$ of bm-600h-GdN plotted vs the frequency ν (closed circle). The solid line represents the best-fitting result using $T_f(\nu)=T_0e^{-a/(\nu+b)}$ with $T_0=23.68$ K, $\alpha=3.5$ Hz, and $b=38$ Hz.

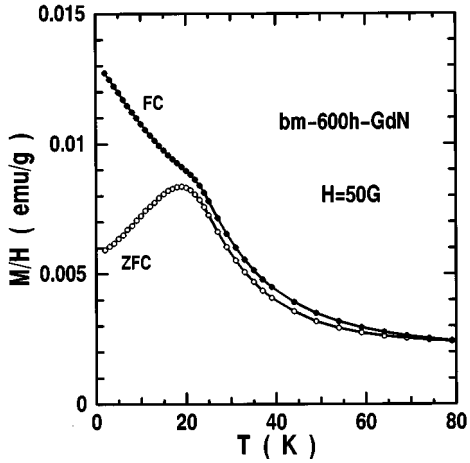

FIG. 5. M/H vs T curves for bm-600h-GdN after zero-field cooling (ZFC) and field cooling (FC) measured in a field of 50 G.

with $T_0=23.68$ K, $a=3.5$ Hz, and $b=38$ Hz, as shown by the solid line in Fig. 4.

Another important feature of all spin glasses is that the dc susceptibility strongly depends on the magnetic history (or irreversibility) below T_f, (i.e., the difference between the zero-field-cooled (ZFC) and field-cooled (FC) magnetizations. This difference is clearly observed in our bm-600h-GdN sample as illustrated in Fig. 5. The M/H gives the initial ac susceptibility when the applied fields are so small that magnetization is roughly proportional to the susceptibility. For the ZFC measurement, the sample was cooled in the absence of an external magnetic field from $T=300$ K to $T=2$ K. Then a field of 50 G was applied and the magnetization was measured as a function of increasing temperature. For the FC measurement, the sample was cooled in the presence of magnetic field $H=50$ G from $T=300$ K to $T=2$ K. Then the magnetization was measured as a function of increasing temperature under this field. At sufficiently high temperatures (above 75 K) a typical paramagnetic behavior is observed: there is no difference between ZFC and FC magnetization. Below 75 K, the ZFC magnetization starts to deviate from the FC magnetization, and below $T_f=19$ K, this irreversibility is more marked. The ZFC curve exhibits a characteristic cusplike maximum at T_f, while the FC curve only exhibits a kink at T_f. For the FC magnetization, the measurement is reversible. This is in contrast to the ZFC magnetization. After applying a field at a temperature below T_f, the ZFC magnetization jumps to a finite value followed by a slow additional increase. This irreversible contribution to χ_{ZFC} decays very slowly if the field is suddenly switched off, as explained later.

It is also a characteristic feature of spin glasses that the temperature of cusplike maximum appearing in ac or dc susceptibility curves is very sensitive to the external magnetic field. The M/H vs T curves (ZFC) of bm-600h-GdN in different external dc magnetic fields are given in Fig. 6. A cusplike maximum similar to that in the ac susceptibility is evident when measuring in a low field. With increasing the applied field, this maximum shifts to a lower temperature and the value of M/H decreases. Under $H=2$ G, the maximum is observed at 20 K, which shifts to 2 K under $H=5$ kG and disappears when the field is higher than 5 kG.

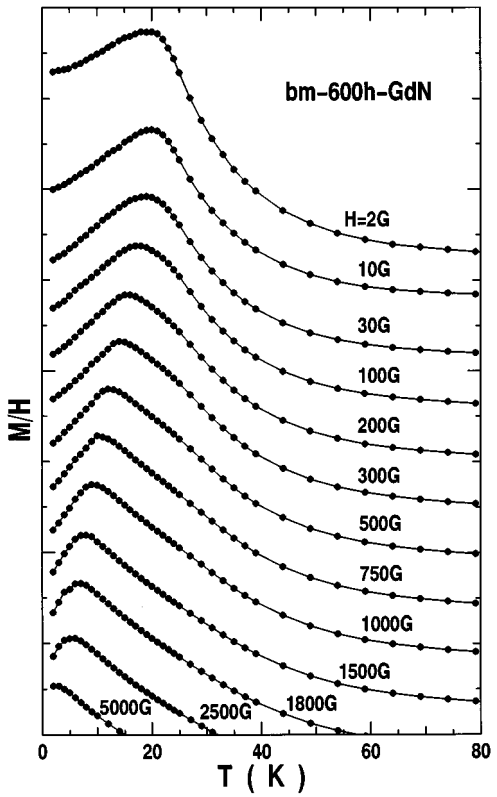

FIG. 6. M/H vs T curves (ZFC) for bm-600h-GdN measured in various dc magnetic fields.

The other important characteristic feature of spin glasses is the existence of remanence and magnetic relaxation on the macroscopic time scale when changing the magnetic field below T_f. This is also observed clearly in our bm-600h-GdN sample. Figure 7 shows the time decay of remanence for bm-600h-GdN measured at different temperature below T_f. This measurement was carried out as follows. The sample was first cooled from a temperature much higher than T_f in zero field to the desired temperature, then a magnetic field of 1 T was applied for about 5 min. After switching off the magnetic field, the remanent magnetization was measured as a function of time. It is clear from this figure that the remanent magnetization of bm-600h-GdN decays so slowly with time t that a nonzero remanence is observed over 3 h. The decay rate is a function of temperature T and the time-dependent remanent magnetization $M(T,t)$ can be fitted very well by the following equation:

$$M(T,t)=M_0(T,\infty)+\alpha(T)/(1+t)+\beta(T)\exp[-t/\tau(T)], \tag{2}$$

where $M_0(T,\infty)$, $\alpha(T)$, $\beta(T)$, and $\tau(T)$ are the fitting parameters which depend only on the temperature. At a fixed temperature, $M_0(T,\infty)$ is a constant representing the remanence value extrapolated to an infinite time. $\alpha(T)$ indicates the main part of the remanence difference between $t=0$ and $t\rightarrow\infty$, because the coefficient $\beta(T)$ is much smaller than $M_0(T,\infty)$. $\tau(T)$ represents an average relaxation time. The best-fitting results obtained by using the least-squares method are shown as the solid lines in Fig. 7 and the fitting parameters are listed in Table I. The values of M_0, α, and β decrease with increasing temperature, while τ is almost

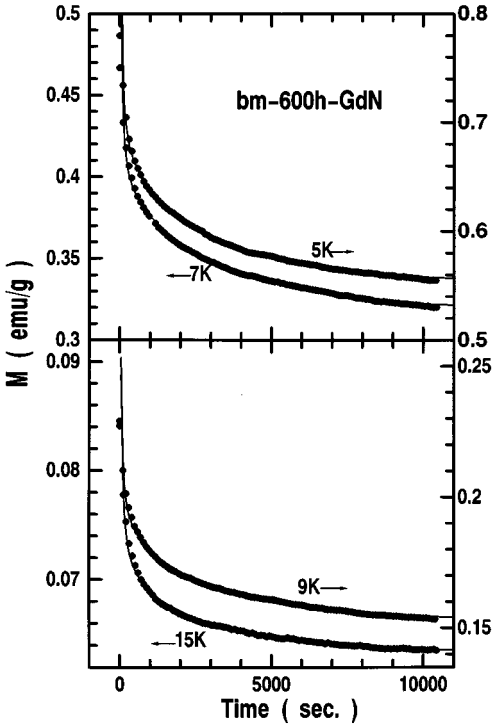

FIG. 7. Decay of remanence as a function of time in bm-600h-GdN measured at different temperatures. The solid lines represent the best fitting results by using the least-squares method.

independent of the temperature in the temperatures of $5\leqslant T\leqslant 15$ K for the bm-600h-GdN sample. The second term in Eq. (2) is important only at the short time scale. The relaxation of the remanent magnetization for bm-600h-GdN shows reciprocal dependence on t at the short time scale. With increasing t, the second term contribution becomes smaller, and the decay law of remanent magnetization of bm-600h-GdN for $t>10$ min can be described by an exponential term as observed for $Au_{100-x}Fe_x$.[18] It is worthwhile noting that there exists a lot of experimental data on the magnetic relaxation behavior of spin glasses and various equations corresponding to different samples are used to fit these data.[19] This suggests that perhaps not all spin-glass properties are universal and that the glasslike structure might vary in its details from system to system.

IV. DISCUSSION

The present results shown above prove that bm-600h-GdN undergoes a single paramagnetic to spin-glass transition with a freezing temperature of about 21.7 K (defined by the peak temperature in the ac susceptibility measured under $\nu=0.01$ Hz) upon cooling from room temperature to lower

TABLE I. ''Best-fit'' parameters of Eq. (2) for the decay of remanence with the time of the bm-600h-GdN sample measured at different temperatures using the least-squares method.

T (K)	M_0 (emu/g)	α (emu sec/g)	β (emu/g)	$\tau(10^3$ sec)
5	0.55	9.38	0.11	3.01
7	0.32	5.78	0.07	3.01
9	0.15	3.14	0.03	3.01
15	0.06	1.06	0.01	3.00

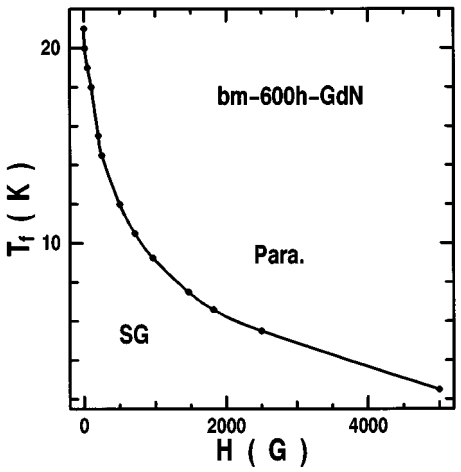

FIG. 8. The T_f vs H phase diagram for bm-600h-GdN. The closed circles denote the peak temperatures in dc magnetization measurements.

temperatures. The freezing temperature T_f shifts to lower temperature with increasing the magnetic field. Using the dc magnetization data measured under different fields (see Fig. 6), the T_f vs H phase diagram is established and displayed in Fig. 8. At the lower magnetic-field region, the Néel temperature T_N of a long-range-order Heisenberg antiferromagnet slightly decreases with increasing H, while in spin glasses the decrease of T_f is marked. We have reported that the initial compound GdN is a ferromagnet with $T_C = 58$ K, and the T_C value does not change even in a magnetic field of 1 T.[17] Thus, the change in T_f of bm-600h-GdN at the lower field region (Fig. 8) represents the intrinsic feature of spin glasses.

Note that the spin-glass behavior of compound GdN is observed only in the samples after ball milling. One question is, what happens in the milled samples? First, ball milling will introduce atomic disorder. This is believed to be the main reason for the spin-glass behavior in bm-GdN milled for more than 10 h. Several impurities (mainly Fe atoms) can infiltrate into the samples in the milling stage. However, their effects on the spin-glass state are considered to be small, because the x-ray diffraction patterns and magnetic properties are restored after annealing the bm-GdN samples to the original phases. The Fe contamination from the milling tools seems to behave superparamagnetically, and this superparamagnetic effect is also weak, as explained later. On the other hand, using a dc sputtering method, we have also prepared the GdN film samples with almost no iron and low oxygen impurity. By controlling the temperature of the substrate, we obtained a sample whose x-ray diffraction patterns are similar to that of the bm-600h-GdN sample, indicating the similarity in structure for them. The ac and dc susceptibility measurements also clearly show the spin-glass behavior for this film sample. Thus, the impurity effect on the spin-glass states in bm-GdN must be small. Recently, Kasuya and Li[20] discussed the strong ferromagnetism in the starting compound GdN originating from the cross processes between the f-d mixing and f-d exchange interactions. For GdN with the NaCl structure, since N atoms are located in the positions between the nearest-neighbor Gd atoms, this mechanism gives a positive magnetic coupling between nearest-neighbor Gd atoms at low temperatures, and the next-nearest-neighbor one is rather weak. Ball milling introduces atomic disorder, but preserves the original crystalline structure, leading to the random occupation of Gd and N atoms on the two crystalline sites. Thus, at low temperatures, the Gd-N-Gd nearest-neighbor interactions are positive, favoring parallel alignment of the Gd magnetic moments, and the Gd-Gd ones are negative, favoring antiparallel alignment of the moments; no unique spin configuration is favored in this case. The competition between the ferromagnetic and antiferromagnetic interactions leads to the formation of a spin-glass state in the bm-GdN samples at low temperature.

It should be noted that the ZFC and FC curves in Fig. 5 do not coalesce even above the spin-glass transition: the FC data lie slightly above the ZFC data up to 75 K. This is partly due to experimental inaccuracy. However, since such irreversibility has not been observed in other spin-glass systems, we have to take into account Fe contamination from the milling tools: Fe impurities cause a superparamagnetic contribution, leading to irreversibility between the ZFC and FC magnetization curves above T_f.[21] Indeed, the simple paramagnetic to spin-glass transition is observed only for the samples milled for $10 \leqslant t \leqslant 1000$ h. After 1530 h of milling, when the sample becomes amorphous, its magnetic behavior is very complicated. In order to check the role of Fe contamination, the bm-1530h-GdN sample was annealed at 800 °C for 72 h. The dc magnetization curves at a field of 10 G before and after annealing show more marked irreversibility, and thus the superparamagnetic behavior is ascribed to Fe contamination. In Fig. 5, however, the irreversibility between the ZFC and FC magnetization curves above T_f is rather small, and therefore the effect of Fe impurities seems to be weak in the bm-600h-GdN sample. Detailed results of superparamagnetism originating from Fe impurities will be discussed elsewhere.

In conclusion, a concentrated binary spin glass, crystalline GdN has been obtained by high-energy ball milling, in which the magnetic element Gd concentration is as high as 50 at. %. This is even higher than that in the first ball-milled crystalline spin glass, i.e., bm-$GdAl_2$.[5] The discovery of spin-glass behaviors in mechanically milled crystalline GdN is significant. It is again proved that mechanical milling is a powerful nonequilibrium processing technique to synthesize spin-glass materials. Particularly for the alloy systems containing a rather large amount of magnetic element, high energy ball-milling is a useful technique to synthesize their spin-glass states. By controlling the milling conditions, one can synthesize various new magnetic materials with interesting physical properties. Another important significance of the high-energy ball-milling technique is that by using this method, we can drive the high melting point and high vapor pressure compounds, such as GdN, to a spin-glass state (or other complex magnetic states), which can be realized in bulk materials and cannot be obtained by traditional rapid solidification.

ACKNOWLEDGMENTS

The authors wish to thank Dr. K. Takada for his chemical analysis. One of the authors (D.X.L.) appreciates the financial support from the COE program of Tohoku University. This work was partially supported by the Grant-in-Aid for Scientific Research on Priority Area (No. 06244106) given by the Ministry of Education, Science, Culture and Sports, Japan.

*Present address: Oarai Branch, Institute for Materials Research, Tohoku University, Oarai, Ibaraki 311-13, Japan. Electronic address: li@ob.imr.tohoku.ac.jp.

[1] V. Cannella and J. A. Mydosh, Phys. Rev. B **6**, 4220 (1972).
[2] C. A. M. Mulder, A. J. van Duyneveldt, and J. A. Mydosh, Phys. Rev. B **23**, 1384 (1981).
[3] H. Maletta and W. Felsch, Phys. Rev. B **20**, 1245 (1979).
[4] L. E. Wenger and J. A. Mydosh, Phys. Rev. Lett. **49**, 239 (1982).
[5] G. F. Zhou and H. Bakker, Phys. Rev. Lett. **73**, 344 (1994).
[6] Y. F. Chen, W. C. Chou, and A. Twardowshi, Solid State Commun. **96**, 865 (1995).
[7] T. Mizoguchi, T. R. McGuire, S. Kirkpatrick, and J. R. Gambino, Phys. Rev. Lett. **38**, 89 (1977).
[8] K. V. Rao, M. Fähnle, E. Figueroa, O. Beckmann, and L. Hedman, Phys. Rev. B **27**, 3104 (1983).
[9] J. A. Geohegan and S. M. Bhagat, J. Magn. Magn. Mater. **25**, 17 (1981).
[10] G. F. Zhou and H. Bakker, Phys. Rev. Lett. **72**, 2290 (1994).
[11] G. F. Zhou and H. Bakker, Phys. Rev. B **48**, 13 383 (1993).
[12] A. Hasegawa and A. Yanase, J. Phys. Soc. Jpn. **42**, 492 (1977).
[13] P. Wachter and E. Kaldis, Solid State Commun. **34**, 241 (1980).
[14] G. Busch, J. Appl. Phys. **38**, 1386 (1967).
[15] T. R. McGuire, R. J. Gambino, S. J. Pickart, and H. A. Alperin, J. Appl. Phys. **40**, 1009 (1969).
[16] R. J. Gambino, T. R. McGuire, H. A. Alperin, and S. J. Pickart, J. Appl. Phys. **41**, 933 (1970).
[17] D. X. Li, Y. Haga, H. Shida, and T. Suzuki, Physica B **199&200**, 631 (1994).
[18] R. J. Bory and T. A. Kitchens, J. Phys. Chem. Solids **34**, 1323 (1973).
[19] K. Binder and A. P. Young, Rev. Mod. Phys. **58**, 801 (1986).
[20] T. Kasuya and D. X. Li, J. Magn. Magn. Mater. (to be published).
[21] B. J. Hickey, M. A. Howson, S. O. Musa, G. J. Tomka, B. D. Rainford, and N. Wiser, J. Magn. Magn. Mater. **147**, 253 (1995).